

## Oxidation behaviour and phase characterization of titaniferous magnetite ore of eastern India

Saikat SAMANTA, Siddhartha MUKHERJEE, Rajib DEY

Department of Metallurgical and Material Engineering, Jadavpur University, Kolkata-700032, India

Received 18 November 2013; accepted 25 March 2014

**Abstract:** Titaniferous magnetite ore is a kind of symbiotic complex ore which comprises ilmenite, magnetite, hercynite and magnesio-hercynite spinel minerals. The ore collected from eastern India was characterized by XRD, WDXRF, SEM and Mössbauer spectroscopy. The oxidation behaviour of fine ore was investigated by TG-DTA analysis under oxygen atmosphere. Subsequent isothermal oxidation experiments were carried out under oxygen and air atmospheres, holding the samples for different periods of time at different temperatures from 873 K to 1473 K. It was observed that ilmenite phase transformed to hematite and titanium dioxide at lower temperature, whereas ferric-pseudobrookite phase was found at higher temperature. Direct reduction of oxidized sample-coke cylindrical briquettes was successfully achieved for phase transition from titaniferous magnetite to iron and titanium dioxide at 1473 K.

**Key words:** titaniferous magnetite; thermal analysis; phase analysis; oxidation; reduction

### 1 Introduction

Titaniferous magnetite ores (TMO) are found in various countries like Australia, China, Russia, South Africa, and New Zealand, and in Indian states like Karnataka, Maharashtra, Orissa and Jharkhand [1,2]. Titaniferous magnetite ore from eastern India, which contains 48%–49% Fe (total), 10%–25% TiO<sub>2</sub> and 0.3%–2.20% V<sub>2</sub>O<sub>5</sub>, is a source of valuable iron, titanium and vanadium. Titanium and vanadium are very popular alloying elements with multiple significant properties and uses in various industries. New applications of vanadium as vanadium redox and flow battery are now very useful in energy sector and create huge potential in future. Titaniferous magnetite ore has complex geo-chemical characteristics of ilmenite and magnetite phases, and hence its processing and utilization has been a great challenge for researchers in the past few decades. The crystal structure of magnetite is inverse spinel, body-centred cubic and very dense in nature. It is very difficult to reduce by gas-solid reaction in a reactor as the kinetics is very slow. The degree of metallization of magnetite is quite lower in comparison with hematite. The presence of poly-metallic element in the solid solution makes the reduction more difficult. On the

contrary, ilmenite is more stable than ordinary iron oxides (hematite and magnetite) because of the solid solution of iron (II) oxide with titanium dioxide. Further, the reducibility of ilmenite is lower because of the high percentage of impurities like manganese and silicone oxides, and a small quantity of magnesium oxide. It is known that manganese oxide inhibits the reduction kinetics of ilmenite, yielding a lower reducibility. The phenomenon can be well explained by the barrier effect [3]. In titanomagnetite series titanium ions gradually replace Fe<sup>3+</sup> iron in B-sites of magnetite lattice (2Fe<sup>3+</sup> → Fe<sup>2+</sup> and Ti<sup>4+</sup>). TMO ore consists of iron oxides and titanium and impurities, such as MnO, SiO<sub>2</sub>, MgO, Al<sub>2</sub>O<sub>3</sub>, CaO, V<sub>2</sub>O<sub>5</sub>, Cr<sub>2</sub>O<sub>3</sub> and trace others. The ease of reduction of titaniferous ores relative to that of hematite or magnetite has been referred to the literature with the conclusion that the more the titanium presents in the ore, the more difficult its reduction is. Thermodynamic data for the reduction of titaniferous magnetite with hydrogen, carbon monoxide, and carbon show that the equilibria are less favourable than for the corresponding reduction of ferrous oxide.

Considering the difficulties in TMO reducibility, oxidation process can be alternative way to beneficiate the ore by structural modification. Oxidation is a well known eco-friendly technology for liberation of

inter-locking grains in mineral processing. It has been commonly applied to rutile and titanium extraction from ilmenite ore [4–8]. The oxidizing roasting leads to the diffusion of oxygen in the ore matrix, forming simple oxides which are porous due to the breakage of complex network. The oxidation processes of ilmenite ore have added advantages, when compared to commercial technologies like sulphuric acid leaching, chlorination and titanium-rich slag processing. The commercial processes have problems such as large amount of leaching residue, environmental burdens and high energy consumption.

It is already established that the reducibility of magnetite and ilmenite is significantly enhanced by pre-oxidation treatment. On the other hand, it is also well known that the reduction kinetics of magnetite is slower than that of hematite due to its close-packed hexagonal structure. During oxidation, the effective surface area increases and opening of structure takes place, which increases the reduction kinetics. PARK and OSTROVSKI [9] have studied the pre-oxidation effects on the ore structure and reduction behaviour of New Zealand titania-ferous ore. Very recently, CHEN et al [10] worked on a simple oxidation route for preparation of pseudobrookite from Panzhihua raw ilmenite, China. Several researchers have carried out the study on the phase transition characteristic and oxidation mechanism of ilmenite ore [11]. In the present study, TMO ore is a combination of magnetite and ilmenite phase. Here, an attempt has been made to study the oxidation behavior and structural modification of the ore under oxygen and air atmospheres. The oxidized pretreated ore is characterized by XRD and SEM. Finally, the direct reduction behaviour of the oxidized ore–coke briquettes is investigated and characterized.

## 2 Experimental

### 2.1 Materials

Titaniferous magnetite ore was collected from Shaltora area, Bankura district, West Bengal, India. The samples were crushed in primary and secondary crushers up to fine sizes. The crushed ore was subjected to sieve analysis by vibratory sieve shaker using micro precision (BSS standard) sieves. Thereafter, the distribution curve was plotted according to the mass fraction of different fine size fractions. The phases were identified by X-ray diffractometer (XRD, Rigaku Ultima-III, Cu K<sub>α</sub>, 40 kV, 30 mV) and the chemical composition was quantified by wavelength dispersive X-ray fluorescence (WDXRF, MagiX 2424, PANalytical, SuperQ) spectrometer. Mineralogical study was characterized by optical microscope and scanning electron microscope (SEM, JEOL JSM-8360). The distribution of different valance

states of iron was investigated by Mössbauer spectroscopy (PC based, constant acceleration mode, 25 mCi <sup>57</sup>Co in Rh matrix, high purity iron foil (12 μm), least squares fitting program LGFIT2).

### 2.2 Thermal analysis

The oxidation behaviour of titaniferous magnetite ore was investigated using Pyris Diamond thermo gravimetric-differential thermal analysis (TG-DTA, PerkinElmer). The fine α-Al<sub>2</sub>O<sub>3</sub> powder was used as reference material. The fine ore (<75 μm) and the reference sample were weighed accurately and were placed inside the sample and reference cells, respectively. The experiment was carried out under oxygen atmosphere by purging 125 mL/min dry oxygen (99.95%). The data were collected using a PC-based data acquisition and processing system. Mass gain (TGA) was investigated at the heating rate of 10 °C/min (283 K/min) up to 1273 K.

### 2.3 Isothermal heat treatment

The fine samples were treated isothermally in the temperature range of 873 to 1473 K under oxygen and air atmospheres. 10 g of sample (<75 μm) was accurately measured and transferred into an alumina crucible and was subsequently charged in a preheated tube furnace. Dry oxygen (purity 99.95%) was purged (flow rate 125 mL/min) for oxidation experiments and the flow rate was controlled by a standard flow meter. The temperature of the heating zone was recorded using Pt/Rh thermocouple. The mass of the sample before and after experiment was measured to calculate the mass gain due to the oxidation reaction. At 873–1073 K, the samples were isothermally treated for three different periods of time (3, 6, 9 h) under oxygen atmosphere. Considering the economic point of view and industrial application, experiments under oxygen atmosphere were not performed for prolonged duration at higher temperature. At 873–1073 K, the samples were isothermally heat treated for six different periods of time (3, 6, 9, 12, 18, 24 h) and the oxidation experiments were carried out for 3 h at 1173–1473 K under air atmosphere. The morphological analysis of the oxidized samples was performed by SEM and part of the samples was used for XRD analysis for identification of phases.

### 2.4 Reduction

Fine coke (below 104 μm) was taken as a reductant for direct reduction and the proximate analysis of coke is performed by standard method. The oxidized samples were uniformly mixed with binders (molasses, bentonite, water) and coke and subsequently pressed to make cylindrical briquettes. The flow chart of briquettes preparation is shown in Fig. 1. The cylindrical briquettes

were mechanically strong enough to perform reduction experiment. The oxidized ore–coke mixtures contained 10% (mole fraction) excess coke than the stoichiometric amount of carbon necessary to reduce oxides of iron, titanium, aluminum and manganese. The presence of other oxides was low and they were considered to be unaffected under given experimental conditions. Each briquette was 4 g in mass, 8 mm in diameter and about 12 mm in height. Green briquettes were dried at 473 K for 3 h in a drying oven. The solid–solid direct reduction experiments of the dried briquettes were performed in a close reactor at 1473 K for 2 h. Two different types of iron oxide phases were observed after the oxidation treatment, i.e. hematite and pseudobrookite series. The reduction experiments were performed with oxidized samples for six different periods of time at 973 K. The same experiments were performed also for each oxidized sample at 1173, 1273, 1373 and 1473 K for 3 h duration. The morphological features of the reduced samples were observed by SEM and the phases were identified by X-ray diffraction (XRD).

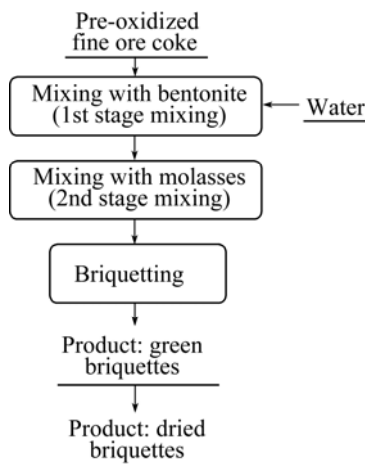


**Fig. 1** Flow chart of briquette preparation

### 3 Results and discussion

#### 3.1 Characterization of ore

Graphical representation of the particle size analysis of the raw ore sample is shown in Fig. 2. It can be observed from the size measurement that the ore is extremely fine and substantial amount of the particle size is below 75  $\mu\text{m}$  (32.18% by mass). Hence, all the oxidation experiments were carried out with the size fraction below 75  $\mu\text{m}$ .

Minerals present in the raw ore were identified by XRD analysis and the result is shown in Fig. 3. Ilmenite ( $\text{FeTiO}_3$ ), magnetite ( $\text{Fe}_3\text{O}_4$ ) and hercynite ( $(\text{Fe}, \text{Mg})\text{Al}_2\text{O}_4$ ) are the major phases. The chemical

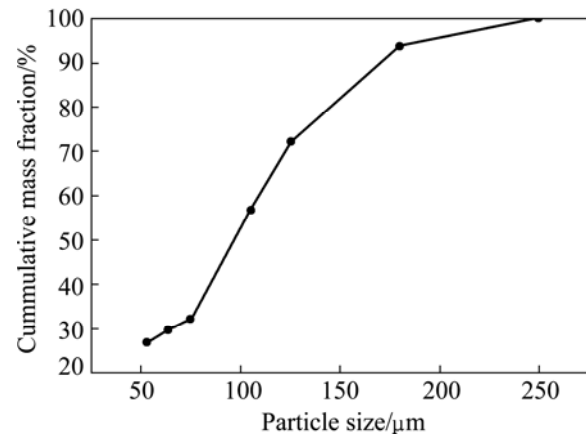


**Fig. 2** Particle size distribution of raw titaniferous magnetite ore

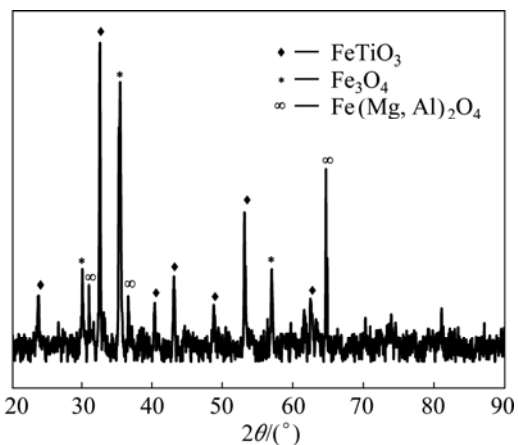


**Fig. 3** XRD pattern of raw titaniferous magnetite ore

**Table 1** WDXRF analysis results of raw titaniferous magnetite ore (mass fraction, %)

Fe <sub>total</sub>	TiO <sub>2</sub>	SiO <sub>2</sub>	Al <sub>2</sub> O <sub>3</sub>	MnO	MgO	CaO
48.18	22.51	1.79	3.37	0.25	1.44	1.12
Na <sub>2</sub> O	P <sub>2</sub> O <sub>5</sub>	V <sub>2</sub> O <sub>5</sub>	K <sub>2</sub> O	Ni	Co	
0.13	0.03	0.435	0.03	0.0341	0.0188	

composition of the sample was analyzed by WDXRF and reported in Table 1. From the table it can be concluded that the ore is highly titaniferous and contains substantial amount of vanadium which makes it economically potential ore. The morphologies and microstructures of the powdered sample and polished sample are shown in Fig. 4. The shapes are angular, sub angular and with various sizes in the powdered sample as shown in Fig. 4(a). The ores are predominantly composed of magnetite, ilmenite, hercynite and magnesio-hercynite minerals and are coarsely interlocked with granular texture. Minor minerals associated are maghemite, rutile, chalcopyrite, chalcocite, cobaltite, gersdorffite, millerite, pseudobrookite and silicates. The associated silicates are mainly

plagioclase and pyroxene. The microstructure of polished sample is shown in Fig. 4(b), which reveals the co-existence of primary grains of well defined magnetite (light phase), ilmenite (dark grey phase), hercynite spinel (dark black phase). Exsolved bodies of hercynite spinel and oxidation-exsolution exsolved lamellae of ilmenite along the octahedral planes (111) and (100) planes are found in most of the large grains, which is a special characteristic of this type of ore [12].

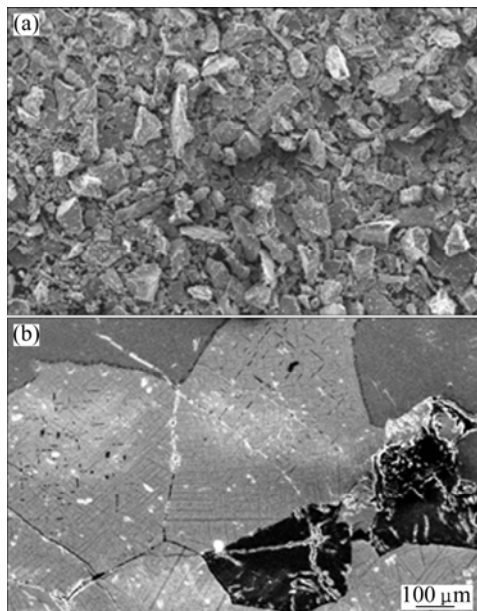


**Fig. 4** SEM micrographs of powdered sample (a) and polished sample (b)

The room temperature Mössbauer spectrum of the sample is fairly complicated, consisting of many lines as shown in Fig. 5. Three sextets and one doublet are fitted to the experimental data to get the best fit. All the hyperfine parameters and relative abundance are tabulated in Table 2. The first sextet in the spectrum having hyperfine field 51.9 T, isomer shift (I.S.) 0.35 mm/s and quadrupole splitting (Q.S.) -0.17 mm/s, is attributed to the presence of pure crystalline hematite ( $Fe^{3+}$ ) phase in the sample [13]. Mössbauer spectrum confirms the presence of magnetite phase having two distinct sites as mentioned in Table 2. The second sextet having hyperfine field of 48.8 T and I.S. 0.37 mm/s is

attributed to the tetrahedral (A) site of magnetite. The third sextet having hyperfine splitting of 46.31 T and I.S. 0.78 mm/s is attributed to the octahedral (B) site of magnetite [14]. The intermediate value of I.S. in Sextet 3 confirms the presence of both  $Fe^{2+}$  and  $Fe^{3+}$  in the octahedral site. Theoretically, in pure magnetite, the tetrahedral (A) site contains  $Fe^{3+}$  and the octahedral (B) site contains both  $Fe^{2+}$  and  $Fe^{3+}$  ions such that the ratio area between these two sites should be 1:2. But the observed non-stoichiometry in this case indicates the presence of some vacancy or presence of foreign elements in the octahedral site. The doublet having I.S. 1.03 mm/s and Q.S. 0.41 mm/s is assigned to ferrous ilmenite.

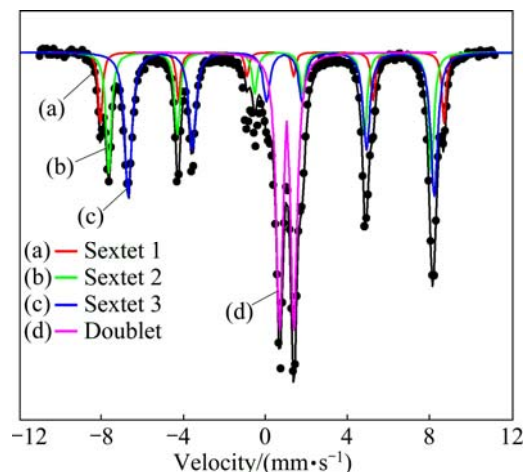


**Fig. 5** Mössbauer spectra of raw titaniferous magnetite ore

The oxidation thermogram of the titaniferous magnetite ore is shown in Fig. 6. In the TGA curve the mass loss step (AB) is extremely minor. In the temperature region of 100 °C (373 K) to 525 °C (798 K), the mass loss is basically due to the loss of moisture and volatile matter in the sample. The mass loss sequence is followed by a mass gain step (BC) until 700 °C (973 K) and after then again a mass gain step (CD) occurs to 850 °C (1123 K). Final mass gain step (DE) is quite higher than the previous steps in the temperature range of 850 °C (1123 K) to 1000 °C (1273 K). The tendency of the curve shows that the mass gain continues due to more pronounced oxidation characteristics.

**Table 2** Mössbauer hyperfine parameters of raw titaniferous magnetite ore

Site	Isomer shift ( $\delta \pm 0.02$ )/ (mm·s <sup>-1</sup> )	Quadrupole splitting ( $2\varepsilon \pm 0.02$ )/ (mm·s <sup>-1</sup> )	Hyperfine splitting ( $H_{int} \pm 0.3$ )/T	Line width ( $\tau \pm 0.002$ )/ (mm·s <sup>-1</sup> )	Sample identification	Relative abundance (RA $\pm 2$ )/%
Sextet 1	0.35	-0.17	51.9	0.24	Ferric	7.29
Sextet 2	0.37	0.04	48.8	0.31	Magnetite A	23.73
Sextet 3	0.78	0.02	46.3	0.41	Magnetite B	35.14
Doublet	1.03	0.41		0.40	Ferrous ilmenite	32.84

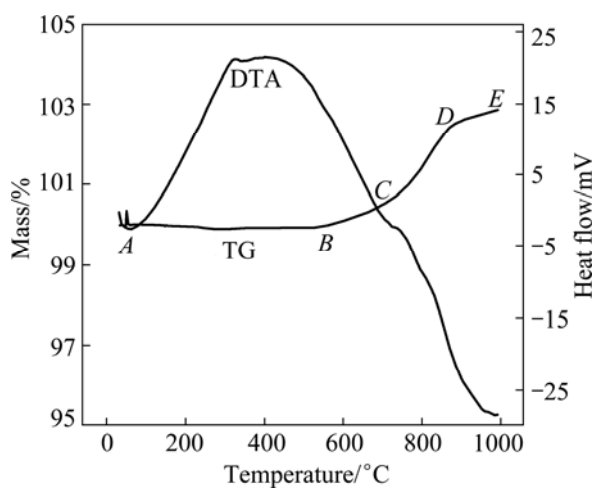


Fig. 6 Thermal analysis of raw ore under oxygen atmosphere

### 3.2 Isothermal treatment of ore

After the oxidation experiment the samples were cooled down to room temperature and then further were ground and used for characterization. Main phase and morphological analysis were investigated in details. Mass gain occurs due to the oxidation of iron from lower state to higher state ( $\text{Fe}^{2+} \rightarrow \text{Fe}^{3+}$ ). The initial mass of the raw sample and its mass gain were recorded to calculate the oxidation conversion of the titaniferous magnetite ore. The oxidation of two  $\text{Fe}^{2+}$  ions to  $\text{Fe}^{3+}$  ions results in one additional  $\text{O}^{2-}$  in the solid product. The degree of oxidation increases with increasing temperature and time. In the presence of pure oxygen, the mineral grains (mainly lower oxidation iron) are diffused with  $\text{O}^{2-}$  ion and getting oxidized. When the duration of oxygen blowing increases, more diffusion occurs; as a result, the effective oxidation becomes higher. The original fine ore is black and changes to brown between 873–973 K due to isothermal oxidation, and with further enhancement of temperature to 1173–1473 K it again changes back to black. The findings of the two experiments under oxygen and air atmospheres are discussed in the following paragraph.

#### 3.2.1 Oxygen atmosphere

All the oxidized samples under oxygen atmosphere were characterized by XRD and SEM for detailed analysis. XRD patterns are shown in Fig. 7. At 873 K, the intensity of ilmenite phase is decreased compared to the raw ore, and simultaneously hematite phase is newly formed. The intensity of hematite phase is increased when the soaking time is enhanced from 3 h to 6 h and ultimately up to 9 h. Whereas at 973 K the ilmenite phase is significantly decreased when compared to 873 K temperature. Here hematite phase becomes the principal phase along with titanium dioxide and magnetite. At 1073 K, ferric-pseudobrookite phase (having small intensity) forms after 3 h of treatment and the intensity of

this phase increases with the increase of soaking time. Ferric-pseudobrookite, titanium dioxide, magnetite and hematite are the dominant phases at this temperature. Major phases found in the oxidation experiment (from XRD patterns) are summarized in Table 3.

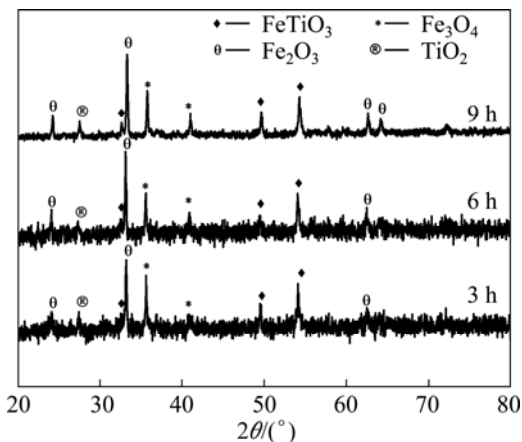


Fig. 7 XRD patterns of oxidized sample at 973 K for different time under oxygen atmosphere

Table 3 XRD analysis results of oxidized samples under oxygen atmosphere

Temperature/K	Oxidation time/h	Phase
873	3	IL, H, M
873	6	IL, H, M
873	9	IL, H, M
973	3	H, M, T
973	6	H, M, T
973	9	H, M, T
1073	3	H, M, T, P
1073	6	H, M, T, P
1073	9	H, M, T, P

\* IL—Ilmenite; H—Hematite; M—Magnetite; T—Titanium dioxide; P—Ferric-pseudobrookite

Morphological study shows special characteristics with eggshell shape on the surface for all treatments under oxygen atmosphere. Some of the micrographs are shown in Fig. 8. In Fig. 8(a), it is observed that the surface of the mineral grain has changed after 3 h of treatment at 873 K under oxygen atmosphere. The same tendency of surface characteristic is found at higher temperature and is shown in Figs. 8(b) and (c).

#### 3.2.2 Air atmosphere

All the oxidized samples under air atmosphere were characterized by XRD and SEM for detailed analysis. The XRD patterns of Indian titaniferous magnetite ore after isothermal oxidation treatment at 873 K under air atmosphere can illustrate the phase evolution of the ore at different time. At 873 K, as the soaking time increases from 3 h to 24 h, ilmenite phase is not observed and the

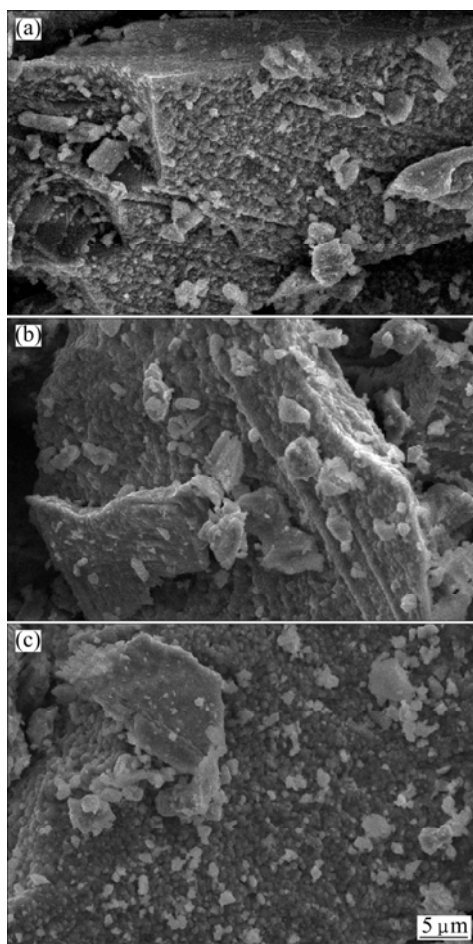


**Fig. 8** Morphologies of oxidized samples under oxygen atmosphere: (a) At 873 K for 3 h; (b) At 973 K for 6 h; (c) At 1073 K for 6 h

hematite phase becomes the dominant phase. After 18 h of oxidation, titanium dioxide ( $\text{TiO}_2$ ) phase is observed along with hematite phase. The intensity of magnetite phase decreases during oxidation treatment. Hematite ( $\text{Fe}_2\text{O}_3$ ) and titanium dioxide ( $\text{TiO}_2$ ) are the phases after oxidation at 973 K from 3 h to 18 h. But at 24 h, there is a ferric-pseudobrookite phase at 973 K. The XRD patterns are shown in Fig. 9. At 1073 K, there is a tendency to form ferric-pseudobrookite ( $\text{Fe}_2\text{TiO}_5$ ) phase. During the phase transformation, the extra ‘Ti’ atom might accommodate into the  $4c$  and  $8f$  sites to the solid solution  $(\text{Fe},\text{Ti})_2\text{TiO}_5$  [15]. Ferric ( $\text{Fe}^{+3}$ ) pseudobrookite has orthorhombic structure. Hematite, ferric-pseudobrookite and titanium dioxide are the phases present after the treatment at 1073 K. The same tendency is observed at the soaking temperatures of 1173 K and 1273 K for 3 h, which is shown in Fig. 10. But ferric-pseudobrookite becomes the principal phase beyond the oxidation temperature 1373 K for 3 h treatment. Major phases found from XRD patterns in oxidation experiment under air atmosphere are summarized in Table 4.

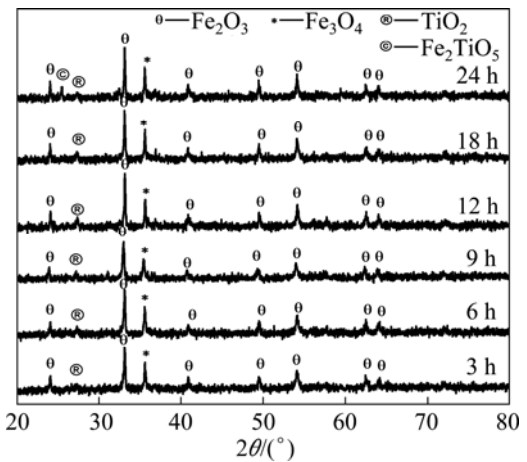


**Fig. 9** XRD patterns of oxidized sample at 973 K for different time under air atmosphere

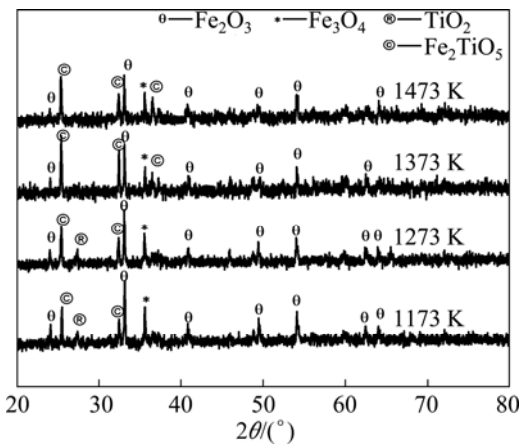


**Fig. 10** XRD patterns of oxidized sample at different temperatures for 3 h under air atmosphere

The SEM characterization was used to study the detailed morphology of the oxidation product. As shown in Fig. 11(a), a gradual growth as eggshell shape is observed at 973 K for 9 h. This structure is identified as ferric oxide, probably hematite. As the soaking temperature increases to 1273 K, the agglomeration of small eggshell shapes starts as shown in Fig. 11(b). At 1473 K, the size of newly formed eggshell is bigger than before (Fig. 11(c)). This might be due to the formation of pseudobrookite phase.

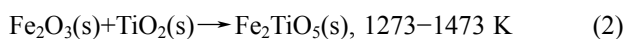
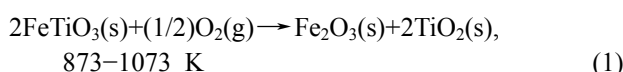
It can be concluded that the effective oxidation of ore in oxygen atmosphere is better than in air oxidation. This is due to the presence of higher partial pressure of oxygen in the reaction zone which significantly enhances the diffusion of oxygen on the surface of mineral. As a result, the phase transformation occurs at lower temperature and time compared to that of air oxidation experiments. Magnetite phase remains even though the ore is oxidized under oxygen and air atmospheres at higher temperature. But the intensity of magnetite phase is decreased at higher temperature. The general oxidation

**Table 4** XRD analysis results of oxidized samples under oxygen atmosphere

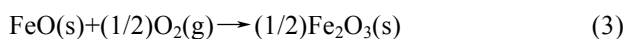
Temperature/K	Oxidation time/h	Phase
873	3	IL, H, M
873	6	IL, H, M
873	9	IL, H, M
873	12	IL, H, M
873	18	IL, H, M, T
873	24	H, M, T
973	3	H, M, T
973	6	H, M, T
973	9	H, M, T
973	12	H, M, T
973	18	H, M, T
973	24	H, M, T, P
1073	3	H, M, T, P
1073	6	H, M, T, P
1073	9	H, M, T, P
1073	12	H, M, T, P
1073	18	H, M, T, P
1073	24	H, M, T, P
1173	3	H, M, T, P
1273	3	H, M, T, P
1373	3	H, M, P
1473	3	H, M, P

IL—Ilmenite; H—Hematite; M—Magnetite; T—Titanium dioxide; P—Ferric-pseudobrookite

reactions can thus be written as



The stoichiometric value of mass gain mainly due to the oxidation of FeO of ilmenite and hercynite spinel to  $\text{Fe}_2\text{O}_3$  in oxidizing atmosphere is calculated from the following reaction



The quantified FeO content in ilmenite phase as well as hercynite phase of Indian titaniferous magnetite is around 23.5%, from which the corresponding stoichiometric mass gain due to the oxidation of FeO is 2.61%. The total mass gain observed from the experiment is close to the calculated percentage in air atmosphere and the deviation might be due to the presence of impurity in the phases.

### 3.3 Reduction

The carbon content of coke is about 80%. According to this analysis the stoichiometric amount of

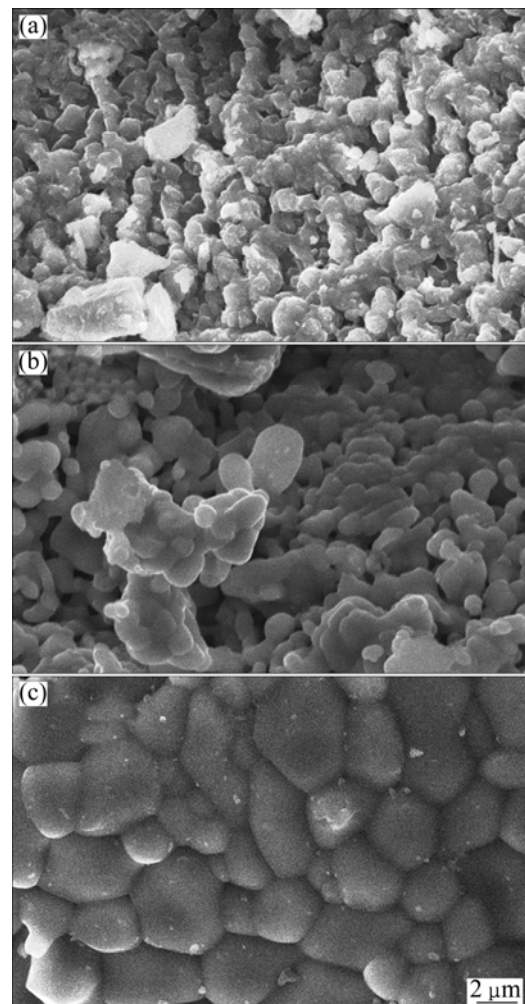


**Fig. 11** Morphologies of oxidized sample under air atmosphere: (a) At 973 K for 9 h; (b) At 1273 K for 3 h; (c) At 1473 K for 3 h

coke is calculated. The dried ore-coke briquettes were isothermally reduced at 1473 K for 2 h in a closed reactor. It is clear that the phase after reduction of six samples (oxidized at 973 K) at 1473 K (time of 2 h) is metallic iron (Fe) as shown in Fig. 12. Very small intensity of ferrous-pseudobrookite phase is present in the XRD pattern. The reaction of the iron bearing phases may be shown as follows.

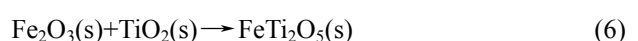
During reduction, hematite is directly reduced to iron.



During reduction, magnetite is also directly reduced to iron.



During reduction, some amount of hematite is agglomerated with  $\text{TiO}_2$  to form ferrous-pseudobrookite ( $\text{FeTi}_2\text{O}_5$ ).



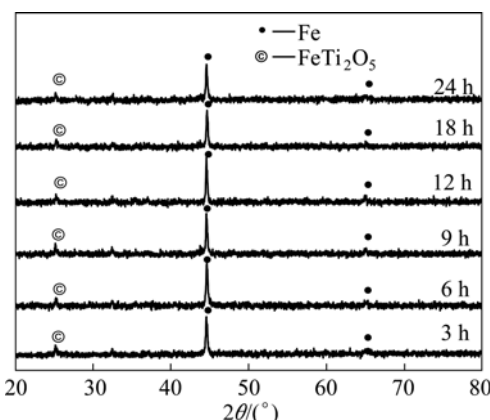


**Fig. 12** XRD patterns of samples (oxidized at 973 K for different time) reduced at 1473 K for 2 h

The XRD analysis of the reduced sample (oxidized at 1173–1473 K) for 2 h is shown in Fig. 13. The observation of different phases in the reduced product of oxidized sample implies that the reduction of hematite and magnetite of briquettes is successfully achieved but the reduction of ferric-pseudobrookite is not easily completed. This may be due to the complex crystallographic structure and slow reduction kinetics of ferric pseudobrookite. Magnetite and hematite phases are totally invisible after 2 h of reduction, and iron and ferrous pseudobrookite ( $\text{FeTi}_2\text{O}_5$ ) are the major phases. Hematite is reduced to wustite ( $\text{FeO}$ ) above 1273 K and then recombines with titanium dioxide ( $\text{TiO}_2$ ) to form stable ferrous-pseudobrookite phase ( $\text{FeTi}_2\text{O}_5$ ). The intensity of ferrous-pseudobrookite of oxidized samples at 1173–1473 K for 3 h is higher than that of the oxidized samples at 973 K for different time. The same inference has been reported by previous researchers [3,16–19].

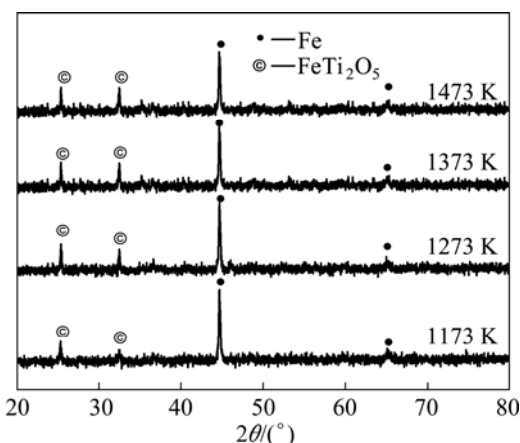


**Fig. 13** XRD patterns of samples (oxidized at 1173–1473 K) reduced at 1473 K for 2 h

The micrographs of samples oxidized at 973 K for 6 h and 12 h are shown in Figs. 14(a) and (b), where a

spongy honeycomb structure is observed with plenty of pores formed. The presence of some unreduced ferrous-pseudobrookite phase is present for the samples oxidized at 1173–1473 K for 3 h. Figure 14(c) shows the unreduced phase of sample oxidized at 1473 K for 3 h. The reduction process is proposed to occur in three steps. Initially, metallic iron particle is formed from magnetite, hematite and ferric-pseudobrookite. Secondly, iron oxides reduction and metallic iron accumulation take place. Finally, the growth of metallic iron particle and formation of polygonal structure occur. All the magnetite, hematite and ferric-pseudobrookite are reduced to metallic iron in the second step. The intimately formed metallic iron is energetically active and is able to assemble and grow. After the growth, metallic iron is eventually liberated from the gangue. Similar observation of iron particles growth from ilmenite reduction has been reported by RANGANATHAN et al [20].

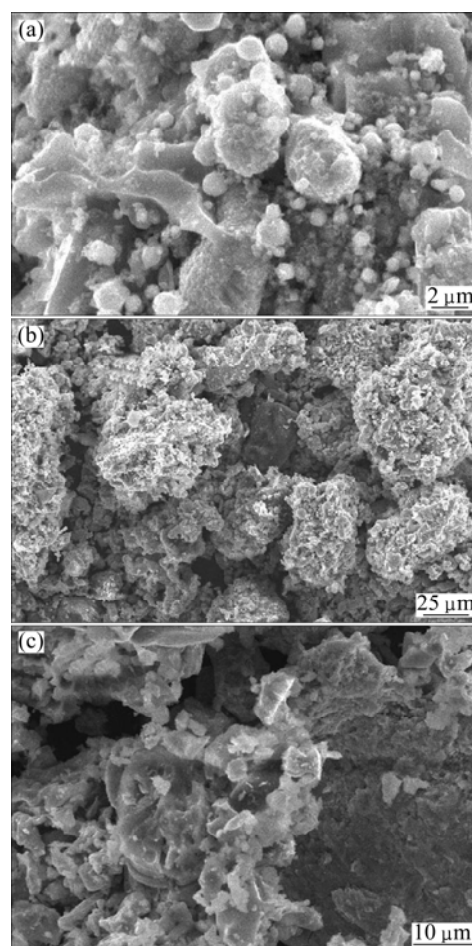


**Fig. 14** Morphologies of reduced briquettes: (a) Oxidized at 973 K for 6 h; (b) Oxidized at 973 K for 12 h; (c) Oxidized at 1473 K for 3 h

#### 4 Conclusions

- 1) Indian titaniferous magnetite ore contains

magnetite and ilmenite as the major iron bearing oxide phases. The contents of  $TiO_2$  and  $V_2O_5$  are 22.51% and 0.435% respectively.

2) In the microscopic study, close interlocking structure of magnetite, ilmenite and hercynite phases and oxidation-exsolution of lamellae of ilmenite are found in the ore. Mössbauer study shows that different percentages of oxidation state of iron ( $Fe^{2+}$  and  $Fe^{3+}$ ) and non-stoichiometry in distribution sites present in the ore.

3) Phase transformation of ilmenite to hematite and titanium dioxide is more effective in the case of oxidation experiment under oxygen atmosphere than under air atmosphere.

4) At lower temperature the major phases are hematite ( $Fe_2O_3$ ), titanium dioxide ( $TiO_2$ ) and magnetite ( $Fe_3O_4$ ), while at higher temperature there is a tendency to form ferrie-pseudobrookite ( $Fe_2TiO_5$ ) phase.

5) The reduction of hematite and magnetite in the oxidized briquettes is successfully achieved at 1473 K for 2 h, but the reduction of ferric-pseudobrookite is difficult to achieve. A new ferrous-pseudobrookite phase is formed after the reduction due to the recombination of wustite and titanium dioxide.

## Acknowledgement

The authors would like to thank Mr. Supratim BISWAS and Mr. Bitan Kumar SARKAR (Research Scholar), Metallurgical & Material Engineering, Jadavpur University, Kolkata, India. We would also like to express our heartfelt gratitude to Mr. S. BHADURI and Mr. Anirban SUR, Chemist, GSI (Eastern Region), Kolkata, India; Dr. D. DAS and S. PATI (Research Scholar) of Mössbauer group, IUC-DAEF, Calcutta Centre, Kolkata, India. One of the authors (Saikat SAMANTA) acknowledges the financial support from Ministry of Steel SDF project, Government of India for funding and providing fellowship.

## References

- [1] MOSKALYK R R, ALFANTAZI A M. Processing of vanadium: A review [J]. *Minerals Engineering*, 2003, 16: 793–805.
- [2] Indian Minerals Year Book 2011. Part II: Vanadium (Advance Release) [M]. Government of India Ministry of Mines. Indian Bureau of Mines, 2012: 2.
- [3] WANG Yu-ming, YUAN Zhang-fu. Reductive kinetics of the reaction between a natural ilmenite and carbon [J]. *International Journal of Mineral Processing*, 2006, 81: 133–140.
- [4] TATHAVADKAR V, KARI C, MOHAN RAO S. Oxidation of Indian ilmenite: Thermodynamics and kinetics considerations [C]// Proceedings of the International Seminar on Mineral Processing Technology. Chennai, India, 2006: 553–558.
- [5] BHOGESWARA RAO D, RIGAUD M. Kinetics of the oxidation of ilmenite [J]. *Oxidation of Metals*, 1975, 9(1): 99–105.
- [6] GUPTA S K, RAJAKUMAR V, GRIEVESON P. Phase transformations during heating of ilmenite concentrates [J]. *Metallurgical Transactions B*, 1991, 22: 711–716.
- [7] ITOH S, SUGA T, TAKIZAWA H, NAGASAKA T. Application of 28 GHz microwave irradiation to oxidation of ilmenite ore for new rutile extraction process [J]. *ISIJ International*, 2007, 47(10): 1416–1421.
- [8] ITOH S, SATO S, ONO J, OKADA H, NAGASAKA T. Feasibility study of the new rutile extraction process from natural ilmenite ore based on the oxidation process [J]. *Metallurgical and Materials Transactions B*, 2006, 37: 979–985.
- [9] PARK E, OSTROVSKI O. Effects of pre-oxidation of titania-ferrous ore on the ore structure and reduction behavior [J]. *ISIJ International*, 2004, 44: 74–81.
- [10] CHEN X, DENG J X, YU R B, CHEN J, HU P H, XING X R. A simple oxidation route to prepare pseudobrookite from panzhihua raw ilmenite [J]. *Journal of the American Ceramic Society*, 2010, 93: 2968–2971.
- [11] FU X, WANG Y, WEI F. Phase transitions and reaction mechanism of ilmenite oxidation [J]. *Metallurgical and Materials Transactions A*, 2010, 41: 1338–1348.
- [12] VIDYASHANKAR H V, GOVINDAIAH S. Ore petrology of the V–Ti magnetite (lodestone) layers of the Kuihndi area of Sargur Schist Belt, Dharwar Croton [J]. *Journal Geological Society of India*, 2009, 74: 58–68.
- [13] NAYAK P K, DAS D, CHINTALAPUDI S N, SINGH P, ACHARYA S, VIJAYAN V, CHAKRAVORTTY V. Quantitative multielemental analysis of titaniferous magnetites by PIXE, EDXRF and their iron mineral characterization by  $^{57}Fe$  Mössbauer spectroscopy [J]. *Journal of Radioanalytical and Nuclear Chemistry*, 2002, 254(2): 351–356.
- [14] CORNELL R M, SCHWERTMANN U. The iron oxides: Structure, properties, reactions. Occurrences and Uses [M]. 2nd ed. Wiley Publishers, 2004.
- [15] GUO W Q, MALAS S, RYAN D H, ALTOUNIAN Z. Crystal structure and cation distributions in the  $FeTi_2O_5$ – $Fe_2TiO_5$  solid solution series [J]. *Journal of Physics: Condens Matter*, 1999, 11: 6337–6346.
- [16] DEWAN M A R, ZHANG G, OSTROVSKI O. Carbothermal reduction of a primary ilmenite concentrate in different gas atmospheres [J]. *Metallurgical and Materials Transactions B*, 2010, 41: 182–192.
- [17] WANG Yu-ming, YUAN Zhang-fu, GUO Zhan-cheng, TAN Qiang-qiang, LI Zhao-ji, JIANG Wei-zhong. Reduction mechanism of natural ilmenite with graphite [J]. *Transactions of Nonferrous Metals Society of China*, 2008, 18: 962–968.
- [18] EL-HUSSINY N. The physic-chemical properties of binderless briquetting of ilmenite concentrate [J]. *The Journal of Ore Dressing*, 2008, 10: 23–29.
- [19] HU T, LV X W, BAI C G, LUN Z G, QIU G B. Reduction behaviour of panzhihua titanomagnetite concentrates with coal [J]. *Metallurgical and Materials Transactions B*, 2013, 44: 252–260.
- [20] RANGANATHAN S, BHATTACHARYYA K K, RAY A K, GODIWALLA K M. Investigation on the reduction and growth of particles of iron from ilmenite ore [J]. *Mineral Processing and Extractive Metallurgy*, 2012, 121: 55–63.

# 印度东部钛磁铁矿的氧化行为和相分析

Saikat SAMANTA, Siddhartha MUKHERJEE, Rajib DEY

Department of Metallurgical and Material Engineering, Jadavpur University, Kolkata-700032, India

**摘要：**钛磁铁矿是一种复杂的共生矿石，含有钛铁矿、磁铁矿、铁铝尖晶石和镁铁铝尖晶石等矿物。对从印度东部采集到的钛磁铁矿石进行 XRD、WDXRF、SEM 和 Mössbauer 谱分析。在氧气气氛下，通过 TG-DTA 分析对矿石的氧化行为进行研究。随后，在氧气和空气气氛下，将样品在不同温度下(873~1473 K)保温不同时间，进行等温氧化实验。观察到在较低的温度下钛铁矿相转变为赤铁矿、氧化钛，而在较高的温度下转变为钛酸亚铁相。将氧化后的矿样与焦炭混合压制圆柱形球团，在 1473 K 下进行直接还原，成功地实现了将磁铁矿铁转变为氧化铁和二氧化钛的相变。

**关键词：**钛磁铁矿；热分析；相分析；氧化；还原

(Edited by Sai-qian YUAN)